

Research Paper

Cytotoxic Effects of the Synthetic Cannabinoid, 5F-MDMB-PICA on Human Glioblastoma U87-MG Cells

Mohammed Mufadhe Alanazi¹✉, Fawaz Alasmari¹, Mohammad M. Algahtani¹, Abdullah S. Alhamed¹, Khaled A. Alhosaini¹, Mohammed M. Almutairi¹, Faleh Alqahtani¹, Wael A. Alanazi¹, Faisal N. Alharbi¹, Raghad Alsanie¹, Mohammed Alshehri¹, Youssef Sari²

1. Department of Pharmacology and Toxicology, College of Pharmacy, King Saud University (KSU), Riyadh, Saudi Arabia.

2. Department of Pharmacology and Experimental Therapeutics, College of Pharmacy and Pharmaceutical Sciences, University of Toledo, Toledo, OH 43606, USA.

✉ Corresponding author: Mohammed Mufadhe Alanazi, Ph.D., Email: momalanazi@ksu.edu.sa; Phone: +966114697639; ORCID ID: 0000-0002-2370-3660.

© The author(s). This is an open access article distributed under the terms of the Creative Commons Attribution License (<https://creativecommons.org/licenses/by/4.0/>). See <https://ivyspring.com/terms> for full terms and conditions.

Received: 2025.09.28; Accepted: 2026.03.27; Published: 2026.04.16

Abstract

Synthetic cannabinoids, particularly 5F-MDMB-PICA, have emerged as potent psychoactive substances, exhibiting a binding affinity to the CB1 receptor approximately 380 times greater than that of Δ^9 -THC, the principal psychoactive compound in cannabis. Their widespread abuse has been associated with severe intoxication and fatalities globally. This study aimed to investigate the cytotoxic effects and mechanisms of 5F-MDMB-PICA in U87-MG astrocyte-like cells, a common model in neurobiological research.

U87-MG cells (passages 7–15) were treated with increasing concentrations of 5F-MDMB-PICA (1–200 μ M) for 24 hours. We employed several assays to evaluate cytotoxicity (MTT assay), oxidative stress, mitochondrial membrane potential, cellular migration (wound healing), and cell death (flow cytometry). Additionally, gene expression analysis via qRT-PCR focused on apoptotic and inflammatory markers. A receptor docking study was performed to verify similarities in binding sites between 5F-MDMB-PICA and Δ^9 -THC.

Our results showed that exposure to 5F-MDMB-PICA led to a concentration-dependent increase in cytotoxicity and oxidative stress, alongside a significant decrease in mitochondrial membrane potential. There was a marked elevation in apoptosis and necrosis, coupled with impaired cellular migration. Gene expression analysis revealed significant upregulation of pro-apoptotic and inflammatory genes, such as P53, Bax, TNF- α , and COX-2, indicating a robust pro-apoptotic and pro-inflammatory response. Notably, key residues (Phe200 and Ser383) in the CB1 binding pocket were identified as crucial for the interaction of both compounds, which might provide insight into the shared patterns of cytotoxic effects.

These findings highlight the neurotoxic effects of 5F-MDMB-PICA, underscoring the serious public health risks associated with synthetic cannabinoids.

Keywords: 5F-MDMB-PICA, U87-MG, neurotoxicity, inflammation, oxidative stress, mitochondrial dysfunction

1. Introduction

Synthetic cannabinoids (SCs) are active substances that mimic the effects of tetrahydrocannabinol (THC), the main psychoactive substance in cannabis, that interact with cannabinoid receptors 1 (CB1) and 2 (CB2). THC acts as a partial agonist of these receptors, whereas synthetic

cannabinoids act as full agonists of both CB1 and CB2. This indicates that they have greater affinity and higher potency for CB1 receptors than THC. Consequently, these compounds can induce considerably stronger harmful effects and exhibit severe toxicity [1]. Cannabinoid receptors are

G-protein-coupled receptors [2]. It has been reported that CB1 receptors are primarily expressed in the central nervous system (CNS), whereas CB2 receptors are primarily expressed in the peripheral systems, particularly the immune system [3]. Historically, SCs were designed, synthesized, and developed in the 1980s to study the effects of endogenous cannabinoids on the brain. They have been linked to aggression, hallucinations, changes in perception and mood, memory impairment, panic attacks, difficulties with concentration, confusion, dizziness, psychosis, slurred speech, and even coma [4]. Furthermore, research indicates that cannabinoids can trigger apoptosis, neuroinflammation, excitotoxicity, and oxidative stress in both *in vitro* and *in vivo* experimental models [5]. For example, Chen et al. have shown that selected SCs can inhibit proliferation and influence both apoptosis and ferroptosis in cellular models [6]. Another study found that certain SCs, such as CUMYL-4CN-BINACA, can trigger apoptosis, generate reactive oxygen species, and induce endoplasmic reticulum stress and inflammation in neuronal tissues [7]. Dogan et al. demonstrated that the SC, Cumyl-4CN-BINACA, induces oxidative stress and activates apoptotic and inflammatory pathways [8]. Additionally, a recent study confirmed that indolic SCs exhibit cytotoxic and antiproliferative effects [9]. Interestingly, a recent study found that both original synthetic compounds (SCs) and their pyrolysis byproducts are classified as neurotoxic substances. These compounds exert their effects by triggering excitotoxicity and activating neuroinflammatory and oxidative stress pathways [10]. SCs are a rapidly growing category of psychoactive substances initially described in patent applications between 2009 and 2011 [11]. Banister et al. evaluated the structure-activity relationships of this subclass of synthetic cannabinoids and synthesized various compounds bearing valine or tert-leucine amide substituents, as well as their methyl ester analogs [11]. 5F-MDMB-PICA (methyl 2-(1-(5-fluoropentyl)-1H-indole-3-carboxamido)-3,3-dimethylbutanoate) (Fig. 1) is a synthetic cannabinoid that is classified as a Schedule I controlled substance by the DEA (Drug Enforcement Administration). It demonstrated the highest potency within this group, with an activity 380 times greater than that of Δ^9 -THC, the main psychoactive compound in natural cannabis. This compound acts via the human cannabinoid receptor subtype (CB1) [11] and is considered the indole analog of the well-known synthetic cannabinoid 5F-ADB (methyl N-([1-(5-fluoropentyl)-1H-indazol-3-yl] carbonyl)-3-methylvalinate). It is commonly found in "legal high" products, such as herbal smoking mixtures [12,13],

vape liquids, or paper products infused with the substance for smuggling into prisons [13,14]. The use of 5F-MDMB-PICA is associated with serious intoxication, overdose, and even increased risk of death [13,15]. It is considered a full agonist that binds to and activates the CB1 receptor, with a high affinity and potency [13]. Activation of this receptor by 5F-MDMB-PICA is associated with agitation, mood swings, confusion, logorrhea, behavioral changes, anxiety, and compulsive-like conditions [15,16]. However, the effects of 5F-MDMB-PICA are not limited to the brain. Exposure to this SC can lead to cardiovascular complications, such as increased heart rate, shortness of breath, and chest pain. In severe cases, SCs can have life-threatening effects on the cardiovascular system, including suppression of cardiac and respiratory functions, circulatory collapse, and cardiac arrest [17]. Owing to the adverse effects of 5F-MDMB-PICA, the United States Drug Enforcement Administration (DEA) placed the substance under emergency Schedule I control in 2019 [18]. This designation indicates that 5F-MDMB-PICA has a high potential for abuse and no accepted medical use, thereby restricting its legal manufacture, distribution, and possession. The widespread presence of 5F-MDMB-PICA in various "legal high" products, its association with serious toxicity and overdose, and its exceptionally high potency, underscore the significant public health threat posed by this synthetic cannabinoid. Thus, the emergency scheduling action of the DEA reflects the urgent need to regulate the availability of this potentially dangerous substance. The biological and toxicological data on the use of SCs are limited, owing to the rapid synthesis and production of these substances. In addition, the pharmacological and toxicological properties of SCs remain largely understudied because these compounds were discovered relatively recently. Therefore, this study aimed to evaluate the modulatory effects of 5F-MDMB-PICA on astrocyte-like U87-MG cells, focusing on cell viability, apoptosis, oxidative stress, mitochondrial function, and inflammation. Our findings may provide insights into the impact of this novel SC on astrocyte-like U87-MG cells and elucidate the mechanisms underlying the harmful effects of 5F-MDMB-PICA on the CNS.

2. Materials and Methods

2.1. 5F-MDMB-PICA Preparation

The SC 5F-MDMB-PICA was generously provided by Dr. Fawaz Alasmari. The compound was solubilized in dimethyl sulfoxide (DMSO) to create a stock solution, which is stored at -20 °C. Various

concentrations of 5F-MDMB-PICA were subsequently prepared directly in the culture medium, as outlined in the cell culture section.

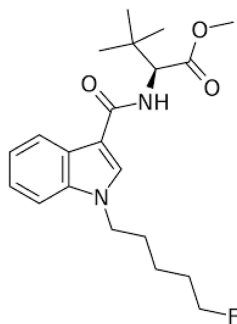


Figure 1: The Chemical Structure of 5F-MDMB-PICA. methyl 2-(1-(5-fluoropentyl)-1H-indole-3-carboxamido)-3,3-dimethylbutanoate.

2.2. Cell Culture

U-87MG human glioblastoma cells (ATCC HTB-14; American Type Culture Collection, Manassas, VA, USA) were cultured between passages 5–9 at an initial density of $\sim 3 \times 10^5$ cells/mL in Dulbecco's Modified Eagle's Medium (DMEM; 1 \times , Gibco®, Grand Island, NY, USA) supplemented with 10% fetal bovine serum (FBS; South American origin, Gibco®) and 1% penicillin-streptomycin (100 U/mL and 100 μ g/mL; Gibco®). Cells were maintained at 37 °C in a humidified 5% CO₂ incubator, with medium renewed every 48 h until reaching ~ 80 –90% confluence. Experiments were conducted using cells at passages 7–15. For functional assays, cells were seeded into 96-well plates for cytotoxicity (MTT; 1×10^4 cells/well, 24 h), reactive oxygen species (ROS; 3×10^4 cells/well, 4 h), and mitochondrial membrane potential (JC-1; 2×10^4 cells/well, 24 h) assessments. In parallel, 6-well plates were used for flow cytometry, polymerase chain reaction (PCR; 1×10^6 cells/well, 24 h), and wound healing (scratch; 3×10^5 cells/well, 24 h) assays. All treatments with 5F-MDMB-PICA were performed in complete culture medium containing FBS and penicillin-streptomycin.

2.3. Cytotoxicity Assay

Cytotoxicity was assessed using the MTT assay as previously described [14]. Briefly, 3-(4,5-dimethylthiazol-2-yl)-2,5-diphenyltetrazolium bromide (MTT; MedChemExpress, USA) was employed to evaluate cell viability and mitochondrial metabolic activity. U-87MG cells were cultured, harvested, and trypsinized as described above, and then seeded into 96-well plates at a density of 1×10^4 cells/well in 100 μ L of complete medium. After 24 h of incubation, cells were treated with various concentrations of 5F-MDMB-PICA (1–200 μ M) for an

additional 24 h. Untreated cells served as the control group (CTRL). Following treatment, 10 μ L of MTT solution (5 mg/mL in phosphate-buffered saline, PBS) was added to each well, and the plates were incubated for 1 h. The resulting formazan crystals were dissolved in 100 μ L of dimethyl sulfoxide (DMSO) with gentle shaking for 5 min, and absorbance was subsequently measured at 570 nm using a microplate reader.

2.4. Oxidative Stress Assay

Intracellular ROS levels were quantified using an H2DCFDA kit (MedChemExpress, USA). This assay is based on the fluorogenic dye 2',7'-dichlorofluorescein diacetate (H2DCFDA/DCF-DA), which passively diffuses into cells and is deacetylated by intracellular esterases to yield a non-fluorescent intermediate. Upon oxidation by intracellular ROS, this intermediate is converted to the highly fluorescent compound 2',7'-dichlorofluorescein (DCF), which exhibits excitation and emission maxima at 485 and 529 nm, respectively. U-87MG cells were seeded in 96-well plates at a density of 3×10^4 cells/well and allowed to adhere for 24 h. Cells were exposed to 200 μ M 5F-MDMB-PICA for 4 hours, a concentration selected based on the MTT assay dose-response curve. Untreated cells were included as the control group (CTRL).

2.5. Mitochondrial Membrane Potential ($\Delta\psi_m$ -JC-1) Assay

Mitochondrial membrane potential was assessed using the JC-1 dye (MedChemExpress, USA), a well-established indicator of mitochondrial function. JC-1 exists in two forms: in healthy, non-apoptotic cells with intact mitochondrial membrane potential, it accumulates in the mitochondria as red-fluorescent aggregates, whereas in apoptotic or depolarized cells it remains in its monomeric green-fluorescent form. U-87MG cells were seeded into 96-well plates at a density of 2×10^4 cells/well and allowed to adhere for 24 h. Cells were then exposed to 200 μ M 5F-MDMB-PICA for 24 hours, a concentration selected based on the MTT assay dose-response curve. Untreated cells were included as the control group (CTRL). Changes in mitochondrial membrane potential were evaluated following the manufacturer's protocol.

2.6. Scratch Assay

The impact of 5F-MDMB-PICA on U-87MG cell migration was assessed using a scratch wound healing assay. U-87MG astrocyte-like cells were seeded and cultured to form a confluent monolayer by overnight incubation. The following day, a linear

scratch was introduced into the monolayer using a sterile 200 μ L pipette tip. Detached cells and debris were removed by replacing the medium, after which cells were treated with 5F-MDMB-PICA at concentrations of 50, 100, or 200 μ M. Untreated cells served as the control group (CTRL). Images of the wound area were captured at 0 and 24 h using an inverted phase-contrast microscope equipped with a charge-coupled device (CCD) camera at 10 \times magnification.

2.7. Flow cytometry

Apoptotic and necrotic cell populations were quantified using annexin V-FITC/propidium iodide (PI) dual staining followed by flow cytometric analysis. U-87MG cells were seeded in 6-well plates at a density of 1×10^6 cells/mL and incubated overnight to allow attachment. Cells were then exposed to 200 μ M 5F-MDMB-PICA for 24 hours, a concentration selected based on the MTT assay dose-response curve. Untreated cells were included as the control group (CTRL). After treatment, cells were harvested by trypsinization, washed with phosphate-buffered saline (PBS) at 25 $^{\circ}$ C, and centrifuged at 1700 rpm for 5 min at 20 $^{\circ}$ C. The resulting pellet was resuspended in 400 μ L of annexin V/PI binding buffer. An aliquot containing approximately 1×10^5 cells in 100 μ L was transferred into 1.5 mL microcentrifuge tubes, followed by the addition of 5 μ L annexin V-FITC and 5 μ L PI. Samples were gently mixed and incubated for 15 min at 25 $^{\circ}$ C in the dark. After incubation, 400 μ L of 1 \times binding buffer was added to each tube, and the samples were analyzed within 1 h using a BD Accuri C6 flow cytometer. The proportion of viable cells was calculated by subtracting the percentage of annexin V-positive (apoptotic) and PI-positive (necrotic) cells from the total cell population.

2.8. Quantitative Real-Time Polymerase Chain Reaction

Total RNA was isolated from U-87MG astrocyte-like cells following treatment with 5F-MDMB-PICA at concentration of 200 μ M for 24 h. Untreated cells served as the control group (CTRL). RNA extraction was performed using TRIzol reagent (Invitrogen/Life Technologies, Carlsbad, CA, USA) according to the manufacturer's protocol. Complementary DNA (cDNA) was synthesized from the extracted RNA using the Reverse Transcription Master Mix for qPCR (MedChemExpress, USA). Quantitative real-time PCR (qPCR) was subsequently carried out using Low ROX SYBR Green qPCR Master Mix (MedChemExpress, USA) and gene-specific forward and reverse primers targeting Bax, P53, COX-2, TNF- α , and the reference gene glyceraldehyde-3-phosphate dehydrogenase

(GAPDH). Primers were obtained from Integrated DNA Technologies (Leuven, Belgium), and their sequences are provided in Table 1. Gene expression levels of Bax, P53, COX-2, and TNF- α were normalized to GAPDH expression, and relative mRNA levels were calculated using the $2^{-\Delta\Delta CT}$ method.

Table 1: Forward and reverse primer sequences

No.	Gene Symbol	Forward Primer Sequence	Reverse Primer Sequence
1	<i>Bax</i>	5'-GTTTCATCCAGGATCGA GCAG-3'	5'-CATCTTCTTCCAGATG GTGA-3'
2	<i>P53</i>	5'-CCCCTCCTGGCCCTGTG ATCTTC-3'	5'-GCAGCGCCTCACAAAC CTCCGCAT-3'
3	<i>TNF-α</i>	5'-CTCTTCIGCTGCACTTT G-3'	5'-ATGGGCTACAGGCTTG TCACTC-3'
4	<i>COX-2</i>	5'-CCCTGGGGTGTCAAAGG TAA-3'	5'-GCCCTCGCTTATGATC TGTC-3'
5	<i>GAPDH</i>	5'-GCCAAGGTCATCCATGA CAACT-3'	5'-GAGGGGCCATCCACA GTCIT-3'

2.9. Protein Preparation

The 3D coordinates of human cannabinoid receptor 1 (CB1) (PDB ID: 8GHV) was obtained for further analysis from Protein Data Bank (PDB) (<https://www.pdb.org/pdb>). This structure, resolved at 2.8 \AA , was initially reported by Kumar et al. (2023) [19]. To prepare the protein (chain D of the CB1) for molecular docking, all heteroatoms, including water molecules, ions, and any ligands, were systematically removed. Energy minimization of the pre-processed protein was performed using Chimera software version 1.13.1 (<https://www.cgl.ucsf.edu/chimera/>). This step is crucial to eliminate any unfavorable interactions that could interfere with molecular docking [20].

2.10. Preparation of Compounds for Molecular Docking against CB1 Receptor

PubChem, a comprehensive chemical database affiliated to the National Center for Biotechnology Information (NCBI) (<https://cactus.nci.nih.gov/translate/>), provided the 3D conformers for Δ 9-Tetrahydrocannabinol (Δ 9-THC) and 5F-MDMB-PICA. The structures of compounds were optimized using Open Babel (<https://openbabel.org/index.html>), an open-source program integrated into the Python Prescription environment. The optimization process utilized the Merck Molecular Force Field (MMFF94), which is well known for its precision in predicting the energies and geometry of organic molecules [21].

2.11. Molecular Docking of Δ^9 -THC and 5F-MDMB-PICA against CB1 Receptor

Molecular docking was performed using Auto Dock Vina to identify potential poses and orientations of compounds, along with their binding energies (BE) at the CB1 binding site [22]. The molecular interaction fingerprints of the compounds were visualized using PyMOL© Molecular Graphics (version 2.4, 2016, Schrödinger LLC, New York, NY, USA) (Seeliger & De Groot, 2010) and BIOVIA's Discovery Studio (version 2016). This analysis highlighted key molecular interaction fingerprints, including hydrogen bonds, hydrophobic interactions, and electrostatic linkages between the CB1 amino acid residues and the ligand atoms.

2.12. Statistical Analyses

All data are expressed as the mean \pm standard error of the mean (SEM). Statistical comparisons were conducted using one-way analysis of variance (ANOVA) followed by Tukey's post hoc test. A P value < 0.05 was considered statistically significant. All analyses were performed using GraphPad Prism software (version 8; GraphPad Software, CA, USA).

3. Results

3.1. 5F-MDMB-PICA-Induced U87-MG Cytotoxicity

U87-MG cells exposed to a wide range of 5F-MDMB-PICA concentrations (1–200 μ M) for 24 h showed a significant concentration-dependent reduction in cell viability. The lowest concentration reduced the viability of U87-MG cells was 20 μ M ($\sim 15\%$, $P < 0.001$). The most significant reduction in U87-MG cell viability was observed at 50 μ M ($\sim 35\%$, $P < 0.0001$), 100 ($\sim 40\%$, $P < 0.0001$), and 200 μ M ($\sim 50\%$, $P < 0.0001$) of 5F-MDMB-PICA. Therefore, these concentrations were selected for the subsequent experiments (Fig. 2).

3.2. 5F-MDMB-PICA Induced Oxidative Stress in U87-MG Cells

Exposure of U87-MG cells to 200 μ M 5F-MDMB-PICA for 4 h significantly increased ROS production ($\sim 42\%$, $P < 0.0001$) compared with the control group (Fig. 3).

3.3. 5F-MDMB-PICA Disrupted the Mitochondrial Membrane Potential in U87-MG Cells

Treating U87-MG cells with 200 μ M of 5F-MDMB-PICA for 24 h reduced the mitochondrial membrane potential ($\Delta\psi_m$) significantly (34%, $P < 0.0001$), compared to the control group (Fig. 4).

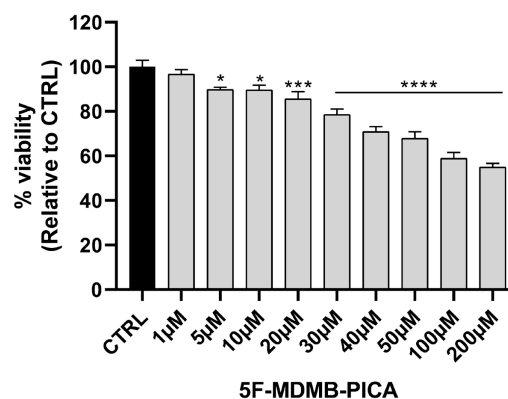


Figure 2: Effects of 5F-MDMB-PICA on U87-MG cell viability. Cells were treated with different concentrations of 5F-MDMB-PICA for 24 h. Cytotoxicity was evaluated using an MTT assay at 570 nm. Data shown as the mean \pm SEM. *** $P < 0.001$ and **** $P < 0.0001$

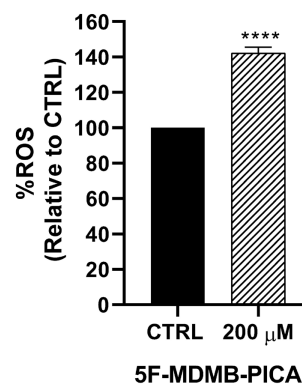


Figure 3: Effects of 5F-MDMB-PICA on the production of reactive oxygen species in U87-MG cells. Cells were treated with 200 μ M 5F-MDMB-PICA for 4 h. ROS generation was evaluated using the DCFDA assay at excitation and emission wavelengths of 485 and 535 nm, respectively. Data are shown as the mean \pm SEM. **** $P < 0.0001$

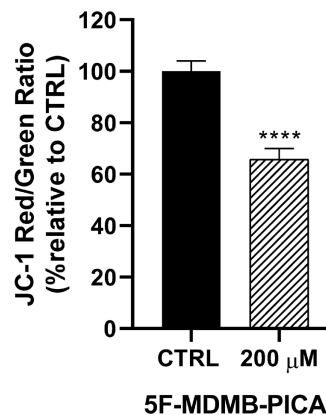


Figure 4: Effects of 5F-MDMB-PICA on the mitochondrial membrane potential of U87-MG cells. Cells were treated with 200 μ M 5F-MDMB-PICA for 24 h. The effect of 5F-MDMB-PICA on $\Delta\psi_m$ was evaluated using the JC-1 assay at excitation and emission wavelengths of (530 or 590 nm, respectively, for the RED oligomers and at 485 or 528 nm for the GREEN monomers). Data are expressed as the mean \pm SEM. * $P < 0.05$, ** $P < 0.01$, and **** $P < 0.0001$

3.4. 5F-MDMB-PICA Reduced U87-MG Cell Migration

The migration of U87-MG cells was impaired in a concentration-dependent manner following 24 h treatment with 50, 100, and 200 μ M 5F-MDMB-PICA.

U87-MG cell migration was significantly inhibited by ~51% ($P < 0.0001$), 65% ($P < 0.0001$), and 80% ($P < 0.0001$) at concentrations of 50, 100, and 200 μM , respectively (Fig. 5).

3.5. 5F-MDMB-PICA Induced Apoptosis and Necrosis in U87-MG Cells

Treating U87-MG cells with 200 μM

5F-MDMB-PICA for 24 h significantly increased apoptosis levels (11-fold, $P < 0.001$) compared to the control group. Interestingly, the necrosis in cells treated with 200 μM 5F-MDMB-PICA was dramatically induced by approximately 90 times ($P < 0.0001$) compared with the control group (Fig. 6).

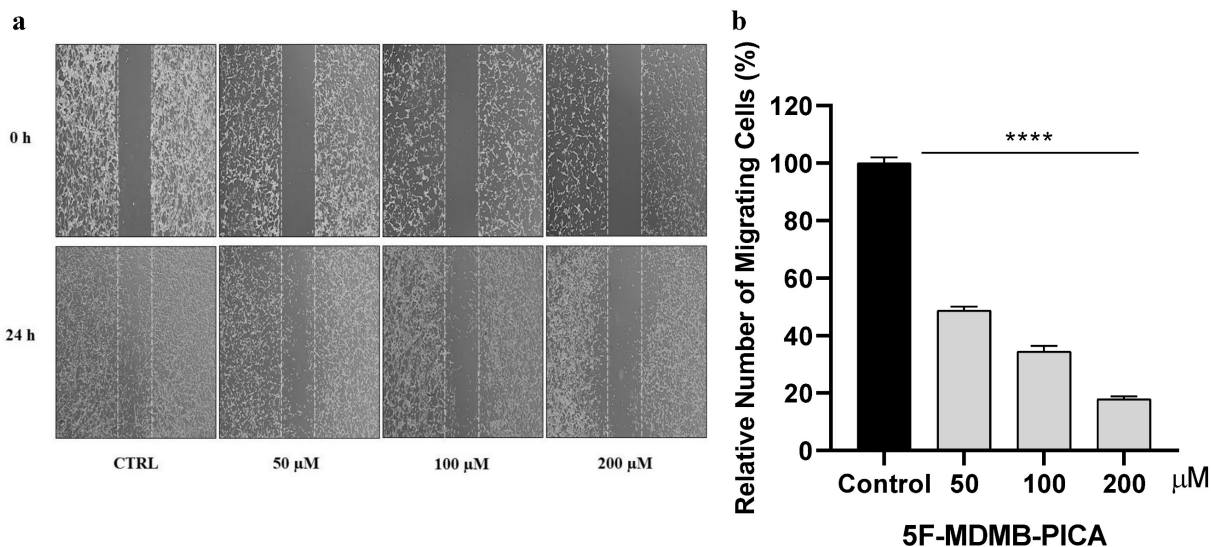


Figure 5: Effect of 5F-MDMB-PICA on U87-MG cell migration. Cells were treated with different concentrations of 5F-MDMB-PICA for 24 h. (a) Representative photomicrograph of U87-MG migration covering the scratch wound area after 24 h of incubation with various concentrations of 5F-MDMB-PICA compared with the control group. (b) The bar graph shows the number of migrated U87-MG cells compared to the control group. Data are expressed as the mean \pm SEM. **** $P < 0.0001$

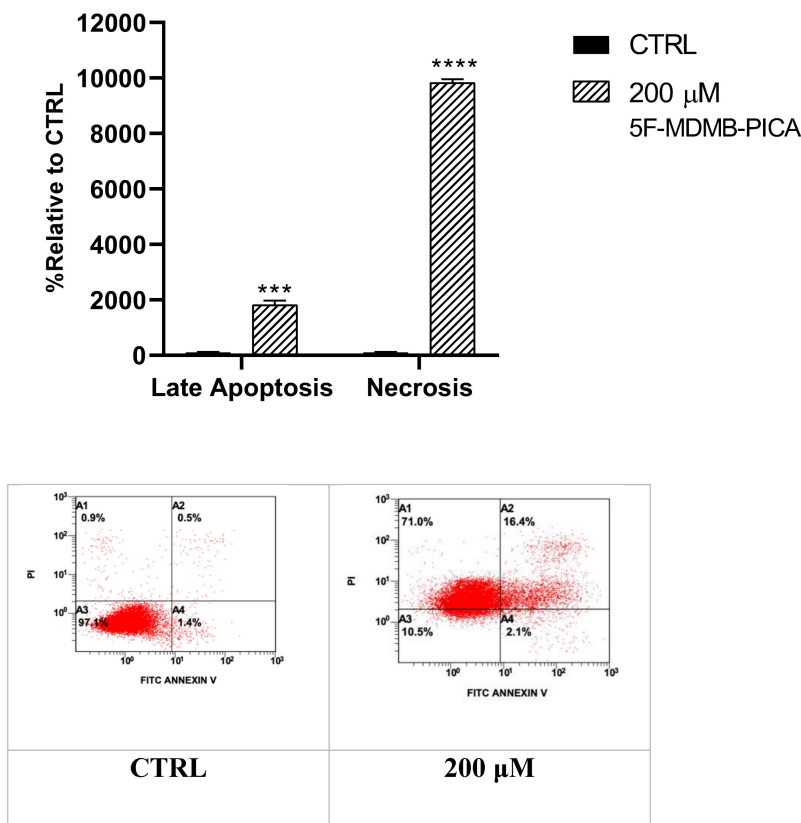


Figure 6: Effects of 5F-MDMB-PICA on the apoptosis and necrosis of U87-MG cells. Cells were treated with 200 μM 5F-MDMB-PICA for 24 h. Apoptosis and necrosis levels were evaluated using annexin V-FITC/PI flow cytometry assay. Data shown as the mean \pm SEM. *** $P < 0.001$ and **** $P < 0.0001$.

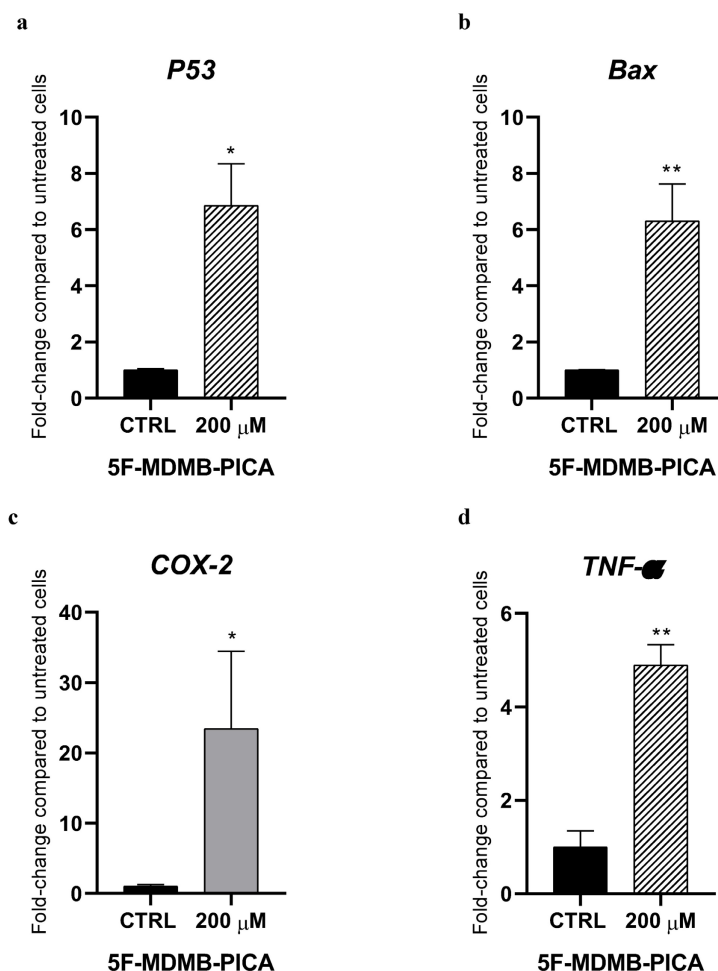


Figure 7: Effects of 5F-MDMB-PICA on the expression of apoptotic and inflammatory genes in U87-MG cells. Cells were treated with 200 μ M 5F-MDMB-PICA for 24 h. *P53* (a), *Bax* (b), *COX-2* (c), and *TNF- α* (d) genes expression were evaluated using qPCR. Data are shown as fold change compared to control group and expressed as the mean \pm SEM. * $P < 0.05$ and ** $P < 0.01$

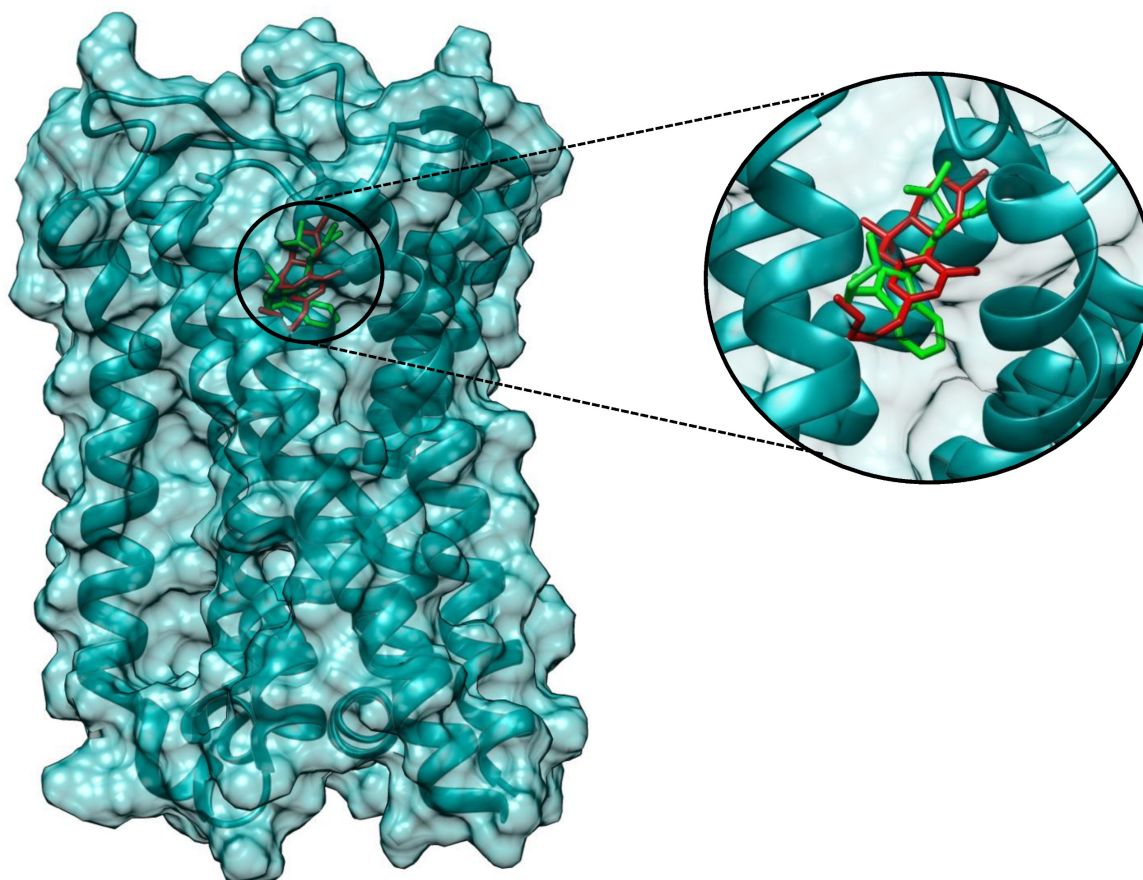
3.6. 5F-MDMB-PICA Modulates the Expression of Pro-Apoptotic and Inflammatory Genes in U87-MG Cells

Treating U87-MG cells with 200 μ M 5F-MDMB-PICA significantly increased the expression of the pro-apoptotic gene *P53* (6-folds) compared with the control group (Fig. 7a). Similarly, expression of the pro-apoptotic gene *Bax* increased significantly following treatment with 200 μ M 5F-MDMB-PICA (6-folds) compared with the control group (Fig. 7b). Moreover, the expression of the pro-inflammatory cyclooxygenase 2 (*COX-2*) increased significantly in U87-MG cells treated with 200 μ M 5F-MDMB-PICA (20-folds) compared with the control group (Fig. 7c). Finally, the expression of pro-inflammatory tumor necrosis factor alpha (*TNF- α*) increased significantly in cells treated with 200 μ M (4.8-folds, $P < 0.01$) compared with the control group (Fig. 7d).

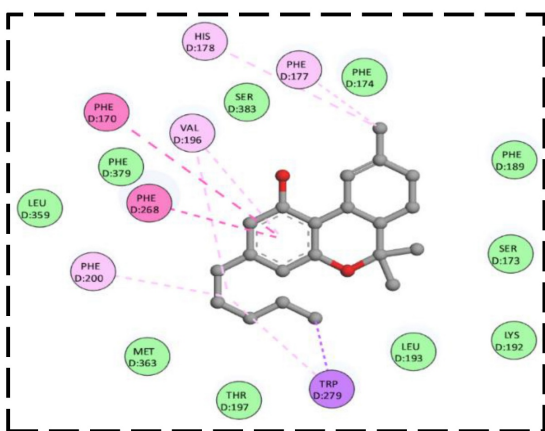
3.7. Analysis of Protein-Ligand Interaction Through Molecular Docking

The binding energy of Δ 9-THC against the CB1 receptor (-10.1 kcal/mol) is comparable to 5F-MDMB-PICA (-8.5 kcal/mol). 2D interaction analysis, showed several residues of the CB1 binding pocket were highlighted as key contributors to Δ 9-THC and 5F-MDMB-PICA (Fig. 8b and c). Among them, Phe200 in both ligands, which has been experimentally validated as essential for ligand binding, where mutational studies have shown that alterations at these positions significantly reduce affinity and impair receptor activity [23]. Ser383 was also identified in the Δ 9-THC and 5F-MDMB-PICA interaction; this residue plays an important role in modulating binding to CB1 [23]. Furthermore, the aromatic cluster, including Phe170 and Phe174, forms a stabilizing microenvironment for CB1 [24]. Additional residues, such as Val196 and Leu193, were found to orient around the ligand, thereby stabilizing CNR1 [24].

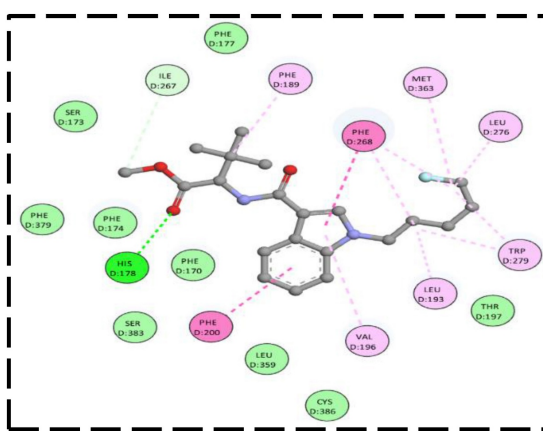
a



b



c



Interactions

- van der Waals
- Conventional Hydrogen Bond
- Carbon Hydrogen Bond
- Pi-Pi T-shaped
- Alkyl
- Pi-Sigma
- Pi-Alkyl

Figure 8: Molecular docking of compounds against CNRI. (a) The 3D binding configuration of THC (Red), 5F-MDMB-PICA (Green). Both ligands occupied similar spots of our protein target. The molecular interaction fingerprints in 2D showed that atoms of THC (b) and 5F-MDMB-PICA (c) interacted with amino acid residues important for binding with CNRI.

4. Discussion

To the best of our knowledge, our study is among the first to investigate the cytotoxic effects of 5F-MDMB-PICA on astrocyte-like U87-MG cells, which serve as a well-established model for examining the effects of both toxic and non-toxic compounds on brain tissue [25]. Additionally, this cellular model (U87-MG) has been found to express the cannabinoid receptor (CB1) [26]. The cytotoxicity of this substance, along with its effects on oxidative stress, mitochondrial function, apoptosis, and inflammation, was evaluated. In this study, 5F-MDMB-PICA induced cytotoxicity in U87-MG cells in a significant, concentration-dependent manner. These results are consistent with those observed in another indole analog of SCs (JWH-018). Sezer et al. [27] showed that JWH-018 significantly decreased the viability of neuron-like SHSY5Y cells. In addition, it induced oxidative stress by decreasing the concentration of the antioxidant glutathione and increasing that of the pro-oxidant malondialdehyde [27]. In another study, the cytotoxic effects of SCs were associated with apoptosis. The harmful effects of SCs have been shown to be mediated by activation of CB-1R, but not of CB-2R [28].

The induction of apoptosis, oxidative stress, and mitochondrial dysfunction biomarkers is associated with numerous neurological disorders and neurodegenerative diseases. Furthermore, it has been implicated in the clinical manifestations and pathophysiology of these diseases, including neuronal loss and behavioral changes [29–31]. Our study confirmed that 5F-MDMB-PICA-induced oxidative stress is concentration-dependent. The correlation among SCs, oxidative stress, and neurotoxicity is well established [27,32]. Activation of the CB1 receptor has been linked to SC-mediated neurotoxicity and oxidative stress [32]. Furthermore, our study demonstrated that 5F-MDMB-PICA induced mitochondrial dysfunction by decreasing $\Delta\psi_m$, an indicator of cytotoxicity and apoptosis. Interestingly, this finding is consistent with previous reports in confirming a correlation between SCs and mitochondrial dysfunction [33]. These results suggest that 5F-MDMB-PICA exposure can lead to harmful manifestations, including aggression, hallucinations, changes in perception and mood, memory impairment, and panic attacks, by inducing neurotoxicity, oxidative stress, and mitochondrial dysfunction.

We further used flow cytometry to confirm whether 5F-MDMB-PICA significantly induces apoptosis and necrosis in U87-MG cells. Our findings demonstrated that the cytotoxic effect of 5F-MDMB-

PICA is associated with the induction of apoptosis and necrosis. Funada et al. [34] have shown that SC-induced neuronal apoptosis occurs via CB1 receptor-mediated caspase-3-dependent pathways. Another study has shown that SCs induced apoptosis, metabolic alterations, and morphological changes in astrocytes [35]. Necrosis has also been reported in association with the use of synthetic cannabinoids [36]. Furthermore, our PCR analyses indicated that 5F-MDMB-PICA enhances the expression of pro-apoptotic and pro-inflammatory genes, specifically Bax, P53, COX-2, and TNF- α . These results provide insight into the possible molecular mechanisms underlying the harmful manifestations of 5F-MDMB-PICA.

Our results correlate with the previous studies that reported the cytotoxic effects of SCs on the CNS [34], [37]. Neuroinflammation and alterations in cannabinoid receptor signaling have been linked to cannabinoid addiction [38]. Furthermore, induction of inflammation by SCs has been associated with the activation of CB1 receptors [39], [40]. Notably, our recently published study revealed that 5F-MDMB-PICA significantly reduced the expression of glutamate transporters in U87-MG cells, including GLT-1, GLAST, and xCT. This suggests that 5F-MDMB-PICA may induce cytotoxicity in U87-MG cells via excitotoxic mechanisms [41]. Finally, migration experiments demonstrated that 5F-MDMB-PICA significantly inhibited U87-MG cell migration in a concentration-dependent manner. This finding is consistent with previous studies showing that cannabinoids can inhibit proliferation and invasion in U87-MG cells. These effects have been linked to those of cannabinoids on ERK1/2 and Akt [42]. Taken together, our study demonstrated the cytotoxic effects of 5F-MDMB-PICA on the CNS. Additionally, these findings provide encouraging data from an oncological perspective, potentially paving the way for future research into the impact of 5F-MDMB-PICA on different cancer cell types. Notably, the anti-tumor activities of SCs have been the focus of considerable research in recent years [43],[44]. Our study has, for the first time, demonstrated that Δ^9 -THC and 5F-MDMB-PICA exhibit overlapping binding residues (Phe200 and Ser383) within the CB-1 receptor pocket. Indeed, since both compounds engage a shared binding site on the CB-1 receptor, this may help elucidate the similarities in their cytotoxic effect patterns. Future studies are warranted to further validate our molecular docking findings through molecular dynamics simulations and binding free energy calculations, which would provide deeper insight into the stability of the ligand-receptor complex and the reliability of the predicted binding

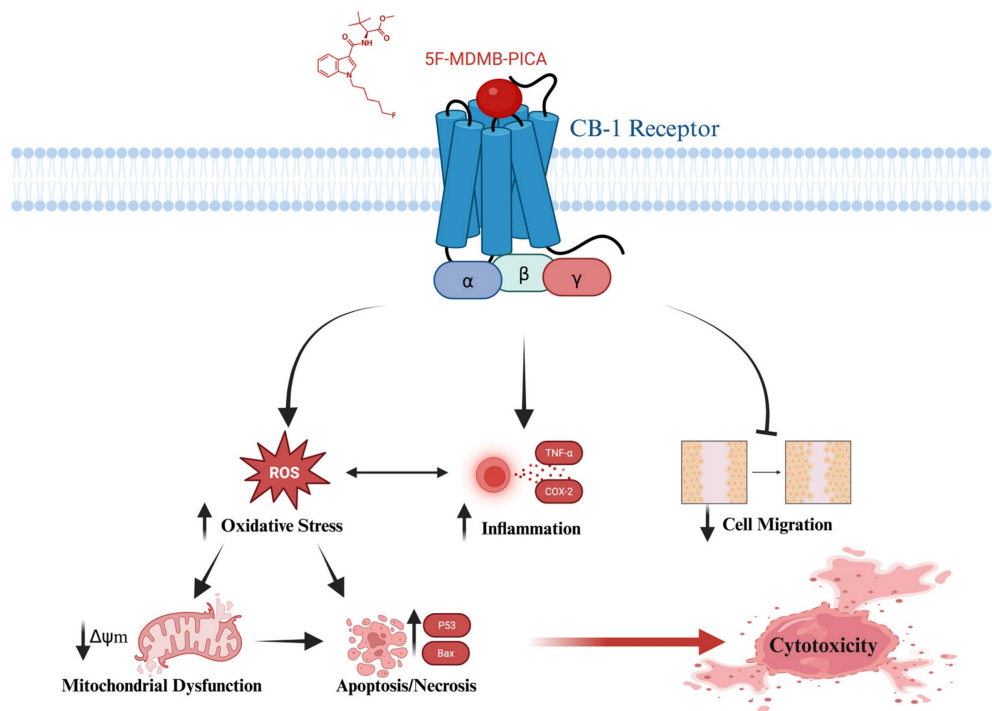


Figure 9. Graphical abstract of the proposed cytotoxic mechanism for the synthetic cannabinoid, 5F-MDMB-PICA on U87-MG cells. Cannabinoid Receptor 1 (CB-1); Reactive Oxygen Species (ROS); Tumor Necrosis Factor- alpha ($TNF-\alpha$); Cyclooxygenase-2 (COX-2); Mitochondrial Membrane Potential ($\Delta\psi_m$); Cellular Tumor suppressor gene (P53); Bcl-2 associated X (Bax).

interactions. Although the present study demonstrates cytotoxic effects of 5F-MDMB-PICA in a human glioblastoma cell line, further investigation in relevant *in vivo* glioblastoma models, followed by clinical studies, is required to assess pharmacokinetics, blood–brain barrier penetration, and translational relevance. Moreover, studies in animal models would enable correlation of the observed cellular effects with *in vivo* and behavioral outcomes associated with 5F-MDMB-PICA exposure. Our study is the first to investigate the effects of 5F-MDMB-PICA on astrocyte-like U87-MG cells.

5. Conclusions

This study provides compelling evidence that 5F-MDMB-PICA induces neurotoxicity through apoptosis, oxidative stress, inflammation, and mitochondrial dysfunction in astrocyte-like U87-MG cells. Also, this study has shown that both Δ^9 -THC and 5F-MDMB-PICA bind to a shared site on the CB-1 receptor. These findings may clarify the mechanisms underlying the harmful effects associated with the consumption of this synthetic cannabinoid (Fig. 9), providing valuable insights into its detrimental impact on health. To the best of our knowledge, our research is the first to present toxicological data regarding the impact and the cytotoxicity mechanisms of 5F-MDMB-PICA on the CNS.

Acknowledgments

Authors acknowledge the support provided by ISU/PNHRC for language editing.

Funding

The authors extend their appreciation to the Ongoing Research Fund program (ORF-2026-1158), King Saud University, Riyadh, Saudi Arabia, for funding this research work.

Data Availability

All data presented in this study are available upon reasonable request from the corresponding authors.

Author Contributions

For research articles with several authors, a short paragraph specifying their individual contributions must be provided. The following statements should be used “Conceptualization M.M.A and F.F.A.; methodology, M.M.A, F.F.A, M.M.A, and A.S.A.; software, M.M.A, K.A.A, F.M.A; validation, M.M.A, F.F.A., A.S.A, and M.M.A.; formal analysis, M.M.A, M.M.A., F.F.A., M.A., and A.S.A.; investigation, M.M.A, M.M.A., M.A., A.S.A.; resources, M.M.A., A.S.A, M.M.A.,W.A.A., and F.F.A.; data curation, M.M.A, M.M.A., M.A., and A.S.A.; writing—original draft preparation, M.M.A., F.N.A., R.A., and F.F.A;

writing—review and editing, M.M.A., F.F.A., F.M.A., W.A.A., F.N.A., R.A., A.S.A., and Y.S.; visualization, M.M.A and M.M.A; supervision, M.M.A.; project administration, M.M.A. and F.F.A; funding acquisition, M.M.A. All authors read and approved the final manuscript.

Competing Interests

The authors have declared that no competing interest exists.

References

- Cooper ZD. Adverse Effects of Synthetic Cannabinoids: Management of Acute Toxicity and Withdrawal. *Curr Psychiatry Rep.* 2017;17(1):100-106. doi:10.1177/0022146515594631. Marriage
- Pál Gyombolai, Dorottya Pap, Gábor Turu, Kevin J. Catt, György Bagdy and LH. Regulation of endocannabinoid release by G proteins: A paracrine mechanism of G protein-coupled receptor action. *Mol Cell Endocrinol.* 2012;353(0):29-36. doi:10.1016/j.mce.2011.10.011. Regulation PubMed PMID: 100000221.
- Pertwee RG. Pharmacology of cannabinoid CB1 and CB2 receptors. *Pharmacol Ther.* 1997 Jan 1;74(2):129-80. doi:10.1016/S0163-7258(97)82001-3 PubMed PMID: 9336020.
- Brunt TM, Bossong MG. The neuropharmacology of cannabinoid receptor ligands in central signaling pathways. *Eur J Neurosci.* 2022;55(4):909-21. doi:10.1111/ejn.14982 PubMed PMID: 32974975.
- Gallegos M SR. Cannabinoids in Neuroinflammation, Oxidative Stress and Neuro Excitotoxicity. *Pharm Anal Acta.* 2015;06(03). doi:10.4172/2153-2435.1000346
- Chen Y, Li H, Liu J, Ni J, Deng Q, He H, et al. Cytotoxicity of natural and synthetic cannabinoids and their synergistic antiproliferative effects with cisplatin in human ovarian cancer cells. *Front Pharmacol.* 2024 Nov 26;15:1496131. doi:10.3389/fphar.2024.1496131
- Eren Demir E, Gur C, Sisman T, Lafzi A, Aksakal Ö. Synthetic cannabinoid CUMYL-4CN-BINACA induces oxidative stress, ER stress, and apoptosis in brain and testicular tissues of male albino rats. *Food Chem Toxicol.* 2025 Oct 1;204:115617. doi:10.1016/j.fct.2025.115617 PubMed PMID: 40618914.
- Dogan T, Aksakal O, Alat O, Halici MB, Gur C. The synthetic cannabinoid CUMYL-4CN-BINACA induces hepatic injury in rats via oxidative stress, NF-κB activation, Nrf2 suppression, EDEM-1, ER stress-mediated apoptotic pathways. *Food Chem Toxicol.* 2026 Jan 1;207:115809. doi:10.1016/j.fct.2025.115809 PubMed PMID: 41109593.
- de Azevedo Cardoso G, de Andrade Querino AL, Silva H, Martins JPA, de Freitas RP, Alves RB. Synthesis, cytotoxicity and QSAR studies of indolic cannabinoid-triazole hybrids. *J Mol Struct.* 2023 Oct 15;1290:135889. doi:10.1016/j.molstruc.2023.135889
- Pita F, Dinis-Oliveira RJ, Silva JP, de Pinho PG, Carvalho F. Neurotoxic potential of synthetic cannabinoids' pyrolysis products. *Toxicology.* 2026 Mar 1;521:154374. doi:10.1016/j.tox.2025.154374 PubMed PMID: 41421516.
- Banister SD, Connor M. The Chemistry and Pharmacology of Synthetic Cannabinoid Receptor Agonist New Psychoactive Substances: Evolution [Internet]. 2018;191-226. doi:10.1007/164_2018_144
- Mogler L, Franz F, Rentsch D, Angerer V, Weinfurter G, Longworth M, et al. Detection of the recently emerged synthetic cannabinoid 5F-MDMB-PICA in 'legal high' products and human urine samples. *Drug Test Anal.* 2017;(February). doi:10.1002/dta.2201
- Glatfelter GC, Partilla JS, Baumann MH. Structure-activity relationships for 5F-MDMB-PICA and its 5F-pentylindole analogs to induce cannabinoid-like effects in mice. *Neuropsychopharmacology.* 2022;47(4):924-32. doi:10.1038/s41386-021-01227-8 PubMed PMID: 34802041.
- Norman C, Walker G, McKirdy B, McDonald C, Fletcher D, Antonides LH, et al. Detection and quantitation of synthetic cannabinoid receptor agonists in infused papers from prisons in a constantly evolving illicit market. *Drug Test Anal.* 2020 Apr 1;12(4):538-54. doi:10.1002/DTA.2767 PubMed PMID: 31944624.
- Kleis J, Germerott T, Halter S, Héroux V, Roehrich J, Schwarz CS, et al. The synthetic cannabinoid 5F-MDMB-PICA: A case series. *Forensic Sci Int.* 2020;314:1-9. doi:10.1016/j.forsciint.2020.110410
- Musa A, Simola N, Piras G, Caria F, Onaivi ES, De Luca MA. Neurochemical and behavioral characterization after acute and repeated exposure to novel synthetic cannabinoid agonist 5-mdmb-pica. *Brain Sci.* 2020;10(12):1-14. doi:10.3390/brainsci10121011
- Tokarczyk B, Jurczyk A, Krupińska J, Adamowicz P. Fatal intoxication with new synthetic cannabinoids 5F-MDMB-PICA and 4F-MDMB-BINACA—parent compounds and metabolite identification in blood, urine and cerebrospinal fluid. *Forensic Sci Med Pathol.* 2022;(0123456789). doi:10.1007/s12024-022-00492-3
- Federal Register: Schedules of Controlled Substances: Temporary Placement of 5F-EDMB-PINACA, 5F-MDMB-PICA, FUB-AKB48, 5F-CUMYL-PINACA, and FUB-144 into Schedule I [Internet]. [cited 2024 Aug 22]. Available from: <https://www.federalregister.gov/documents/2019/04/16/2019-07460/schedules-of-controlled-substances-temporary-placement-of-5f-edmb-pinaca-5f-mdb-pica-fub-akb48>
- Krishna Kumar K, Robertson MJ, Thadhani E, Wang H, Suomivuori CM, Powers AS, et al. Structural basis for activation of CB1 by an endocannabinoid analog. *Nat Commun.* 2023 Dec 1;14(1). doi:10.1038/s41467-023-37864-4 PubMed PMID: 37160876.
- Mackay DHJ, Cross AJ, Hagler AT. The Role of Energy Minimization in Simulation Strategies of Biomolecular Systems. *Predict Protein Struct Princ Protein Conform.* 1989;317-58. doi:10.1007/978-1-4613-1571-1_7
- Halgren TA. Merck molecular force field. I. Basis, form, scope, parameterization, and performance of MMFF94. *J Comput Chem.* 1996 Apr 1;17(5-6):490-519. doi:10.1002/(SICI)1096-987X(199604)17:5<6490::AID-JCC1>3.0.CO;2-P
- Trott O, Olson AJ. AutoDock Vina: improving the speed and accuracy of docking with a new scoring function, efficient optimization and multithreading. *J Comput Chem.* 2010 Jan 30;31(2):455. doi:10.1002/JCC.21334 PubMed PMID: 19499576.
- Sitkoff DF, Lee N, Ellsworth BA, Huang Q, Kang L, Baska R, et al. Cannabinoid CB1 receptor ligand binding and function examined through mutagenesis studies of F200 and S383. *Eur J Pharmacol.* 2011 Jan 25;651(1-3):9-17. doi:10.1016/j.ejphar.2010.10.056 PubMed PMID: 21044623.
- Hua T, Vemuri K, Nikas SP, Wu Y, Qu L, Pu M, et al. Crystal structures of agonist-bound human cannabinoid receptor CB1. *Nat* 2025. 2025 Aug 27;1-5. doi:10.1038/s41586-025-09454-5
- Bakos J, Strbak V, Ratulovska N, Bacova Z. Effect of oxytocin on neuroblastoma cell viability and growth. *Cell Mol Neurobiol.* 2012 Jul;32(5):891-6. doi:10.1007/s10571-012-9799-1
- Giannotti L, Di Chiara Stanca B, Spedicato F, Vergara D, Stanca E, Damiano F, et al. Exploring the Therapeutic Potential of Cannabidiol in U87MG Cells: Effects on Autophagy and Nrf2 Pathway. *Antioxidants* 2025, Vol 14, Page 18. 2024 Dec 26;14(1):18. doi:10.3390/ANTIOX14010018
- Sezer Y, Jannuzzi AT, Huestis MA, Alpertunga B. In vitro assessment of the cytotoxic, genotoxic and oxidative stress effects of the synthetic cannabinoid JWH-018 in human SH-SY5Y neuronal cells. *Toxicol Res (Camb).* 2020;9(6):734-40. doi:10.1093/TOXRES/TFAA078
- Tomiyaama K, Funada M. Cytotoxicity of synthetic cannabinoids found in "Spice" products: The role of cannabinoid receptors and the caspase cascade in the NG 108-15 cell line. *Toxicol Lett.* 2011 Nov 10;207(1):12-7. doi:10.1016/j.toxlet.2011.08.021 PubMed PMID: 21907772.
- Tatton WG, Olanow CW. Apoptosis in neurodegenerative diseases: the role of mitochondria. *Biochim Biophys Acta - Bioenerg.* 1999 Feb;1410(2):195-213. doi:10.1016/S0005-2728(98)00167-4
- Wu Y, Chen M, Jiang J. Mitochondrial dysfunction in neurodegenerative diseases and drug targets via apoptotic signaling. *Mitochondrion.* 2019 Nov 1;49:35-45. doi:10.1016/j.mito.2019.07.003 PubMed PMID: 31288090.
- Kim GH, Kim JE, Rhie SJ, Yoon S. The Role of Oxidative Stress in Neurodegenerative Diseases. *Exp Neurobiol.* 2015 Dec;24(4):325-40. doi:10.5607/en.2015.24.4.325
- Oztas E, Abudayyak M, Celiksoz M, Özhan G. Inflammation and oxidative stress are key mediators in AKB48-induced neurotoxicity in vitro. *Toxicol Vitro.* 2019;55:101-7. doi:10.1016/j.tiv.2018.12.005
- Canazza I, Ossato A, Vincenzi F, Gregori A, Di Rosa F, Nigro F, et al. Pharmacotoxicological effects of the novel third-generation fluorinate synthetic cannabinoids, 5F-ADBINA, AB-FUBINA, and STS-135 in mice. In vitro and in vivo studies. *Hum Psychopharmacol Clin Exp.* 2017 May 1;32(3):e2601. doi:10.1002/HUP.2601 PubMed PMID: 28597570.
- Tomiyaama K ichi, Funada M. Cytotoxicity of synthetic cannabinoids on primary neuronal cells of the forebrain: the involvement of cannabinoid CB1 receptors and apoptotic cell death. *Toxicol Appl Pharmacol.* 2014 Jan 1;274(1):17-23. doi:10.1016/j.taap.2013.10.028
- Cocini T, De Simone U, Lonati D, Scaravaggi G, Marti M, Locatelli C. MAM-2201, One of the Most Potent-Naphthoyl Indole Derivative-Synthetic Cannabinoids, Exerts Toxic Effects on Human Cell-Based Models of Neurons and Astrocytes. *Neurotox Res.* 2021 Aug 1;39(4):1251-73. doi:10.1007/S12640-021-00369-3 PubMed PMID: 33945101.
- Mansoor K, Zawodniak A, Nadasdy T, Khitan ZJ. Bilateral renal cortical necrosis associated with smoking synthetic cannabinoids. *World J Clin Cases.* 2017;5(6):234. doi:10.12998/WJCC.V5.I6.234 PubMed PMID: 28685136.
- Esawy A, Eltablawy N, Abd El-Fattah A, Abdalwahab W. Oxidative Stress, Inflammation and Apoptosis are the Main Mediators in AMB-FUBINA Induced Brain Injury in Male Albino Rats. *Azhar Int J Pharm Med Sci.* 2021;55:1-1-107. doi:10.21608/aijpm.2021.210570
- Rodrigues LCM, Gobira PH, De Oliveira AC, Pelição R, Teixeira AL, Moreira FA, et al. Neuroinflammation as a possible link between cannabinoids and addiction. *Acta Neuropsychiatr.* 2014;26(6):334-46. doi:10.1017/neu.2014.24 PubMed PMID: 25455257.
- Zawatsky CN, Abdalla J, Cinar R. Synthetic cannabinoids induce acute lung inflammation via cannabinoid receptor 1 activation. *ERJ Open Res.* 2020 Jul 1;6(3):1-4. doi:10.1183/23120541.00121-2020 PubMed PMID: 32832534.
- Alzu'bi A, Almahasneh F, Khasawneh R, Abu-El-Rub E, Baker WB, Al-Zoubi RM. The synthetic cannabinoids menace: a review of health risks and toxicity.

- Eur J Med Res. 2024;29(1):1-10. doi:10.1186/s40001-023-01443-6 PubMed PMID: 38216984.
41. Alsulaimi IN, Alanazi MM, Alhosaini KA, Ahamad SR, Khan MR, Almezied FS, et al. Effects of a synthetic cannabinoid, 5F-MDMB-PICA, on metabolites and glutamatergic transporters in U87 cell line. *Neuroscience*. 2025 Jun 21;577:190-9. doi:10.1016/j.neuroscience.2025.05.016 PubMed PMID: 40389124.
 42. Solinas M, Massi P, Cinquina V, Valenti M, Bolognini D, Gariboldi M, et al. Cannabidiol, a Non-Psychoactive Cannabinoid Compound, Inhibits Proliferation and Invasion in U87-MG and T98G Glioma Cells through a Multitarget Effect. *PLoS One*. 2013;8(10). doi:10.1371/journal.pone.0076918 PubMed PMID: 24204703.
 43. Ko MW, Breznik B, Senjor E, Jewett A. Synthetic cannabinoid WIN 55,212-2 inhibits growth and induces cell death of oral and pancreatic stem-like/poorly differentiated tumor cells. *Adv Cancer Biol - Metastasis*. 2022;5(January):100043. doi:10.1016/j.adcanc.2022.100043
 44. Benedicto A, Arteta B, Duranti A, Alonso-Alconada D. The Synthetic Cannabinoid URB447 Exerts Antitumor and Antimetastatic Effect in Melanoma and Colon Cancer. *Pharmaceuticals*. 2022;15(10):1-11. doi:10.3390/ph15101166